Journal of Theoretical and Applied Information Technology
30th September 2021. Vol.99. No 18

ISSN: 1992-8645 www.jatit.org E-ISSN: 1817-3195

MODELING AND SIMULATION OF THE EVOLUTION OF THE CORONA VIRUS PANDEMIC IN A CONTEXT OF MIGRATION

[1,2]SALMA CHABBAR, [1]MOHAMMED BENMIR, [1]JAAFAR EL KARKRI, [1]KHALID BENSAID, [1]RAJAE ABOULAICH, [3]CHAKIB NEJJARI

[1]Laboratory LERMA, Mohammadia School of Engineering, Mohammed V University in Rabat, Avenue Ibn Sina B.P 765, Agdal Rabat 10090, Morocco

[2]Université Côte d'Azur, Inria, CNRS, LJAD, UMR 7351, Parc Valrose, 06108 Nice, France.

[3]Mohammed VI University of health sciences, Anfa City: Bld Mohammed Taïeb Naciri,Commune Hay Hassani 82 403 Casablanca, Morocco

E-mail : [1,2]chabbarsalma@gmail.com, [1]mohammed.benmir-etu@etu.univh2c.ma, [1]elkarkri@emi.ac.ma, [1]bensaid.khalid@gmail.com, [1]aboulaich@emi.ac.ma, [2]cnejjari@um6ss.ma

ABSTRACT

The present article deals with a COVID-19 propagation system. A new compartmental model is established. Migration is allowed into the population. We establish the basic reproduction number and proof that it is an increasing function of migration rates. The final size relation has been determined in the case of closed population. Moroccan data are used in order to compute the parameters of the proposed model. Principal epidemiological results have been compared in the presence and absence of migration using a simulation algorithm based on the dynamical systems approach on the one hand, and the multi-agent approach on the other hand. Both approaches have been implemented using NetLogo. The study, under the two approaches, has proven that migration causes a diminution of the timing of the general infection and the symptomatic peaks. It causes also an augmentation in the maximum values of the general infection and the symptomatic prevalences. The model provides a quantitative illustration of migration influence on disease spread in populations and proposes a practical hybrid framework that will be useful in analyzing and controlling many case studies of COVID-19 spread.

Keywords: *COVID-19 spread, Compartmental models, Ordinary differential equations, Multi-agents simulation, Migration.*

1. INTRODUCTION

In December 2019, the Wuhan Center for Disease Control and Prevention in China's Hubei province reports a cluster of pneumonia cases. A new Corona-virus that will result in a global pandemic was identified. The massive spread of the new discovered Corona-virus disease (Covid-19) led to millions of deaths worldwide so far and took a toll on the global economy. Governments in the face of this pandemic have noticed that very good strategies can be addressed through mathematical modeling of the spread of the disease. Indeed, and as underlined in [1] and [2], these mathematical tools allow scientists and professionals to understand the behavior of the pandemic and its evolution and to study the impact of the various possible political decisions on general health of the population.

Compartmental modeling is an important and efficient tool in representing, forecasting and controlling the behavior of epidemiological systems. The approach consists on dividing the population under study into different sub-populations called compartments [3] and [4].

The analysis of the disease dynamic leads to differential equations governing the infection's outbreak. The nature of the differential equation relates to the assumptions made by the researcher and on the biological properties of the disease under study.

The SIR model is the reference for COVID-19 modeling. It is a three-compartment that divides the

population into susceptible, infected and recovered individuals and many papers have used it to describe the evolution of Covid-19 infection over time [1], [6] and [7]. By adjusting the parameters of the model, many case studies from different countries have been analyzed to provide valuable predictions on COVID-19 spread using the SIR model, such as Italy [1], China, South Korea, India, Australia, USA [6]and different European countries [8]. However, the SIR model, as pointed out by [9], despite providing reasonable forecast in the short term, does not accurately describe the evolution of the disease in the long term. With only three compartments, the SIR model does not fully describe the mechanisms of the Covid-19 spread.

Covid-19 is characterized by an incubation period where the infected individual is not yet infectious and by the appearance of asymptomatic cases where the infected individual is infectious but does not exhibit any symptoms. Hence the relevance of adding two compartments to the basic SIR model to consider the incubation period and the asymptomatic cases. The compartment involving the individuals in the incubation period is often referred to as the Exposed or Latent compartment [2], [10], [11] and [12].

The SIRSi model proposed in [13] offers a fourth compartment for the unreported and asymptomatic cases and was fitted to accommodate the difference in the immunity within a population. In [10], an extended SEIQR model for Covid-19 is presented, where the quarantined and hospitalized compartments are included in addition to the exposed compartment. Different levels of lockdown are investigated in [10] through a coefficient of social interaction and the risk of relapse of the disease is also considered. In [2], by adding a new compartment of semi-susceptible individuals with a better immune system than the susceptible, better results are achieved. A vaccinated compartment is also included in [2] to study the effect of vaccination on the spread of the virus. Covid-19 modeling helps analyzing the effects of different health measures and policies adopted by governments, whether it is vaccination [2], social distancing [13] or restrictions on people' migration [12], [14] and [15].

In [11], Julien Arino and Stéphanie Portet proposed a modified SLIAR model better suited to diseases with a latent period, in addition to symptomatic and asymptomatic outbreaks. Using Erlang distributions in [11] for the sojourn times, description and replacing the L, A and I compartments, each one, by two sub-compartments of the same category of individuals enables a better description of the time period in those critical compartments and thus allows a better modeling of the COVID-19 propagation. In order to have an even better description of the sojourn times, the results achieved in [11] are further extended in the present work by adding a third sub-compartment in each of the Latent, Infectious and Asymptomatic compartments. In addition, the model developed in this paper was adjusted to investigate the effect of migration on the propagation of COVID-19.

Furthermore, in the disease modeling, if we assume that the state at time t doesn't depend on spatial parameters and on the state at the previous times t-ω, then we obtain an ordinary differential equation [16] and [17]. In other contexts, one should include time delay in the model. As pointed out in [4] and [18], for some diseases, if we denote τ the latent period, then the number of infective individuals at time t depends on the number of infective cases at times t-τ, and consequently, the system is governed by a delay differential equation with constant delay. We refer the reader to [3], [4] and [19] for further details. Mathematical analysis provides conditions on the model's parameters under which the system converges to one of its steady states. There are in general two types of steady states: disease free equilibrium corresponding to zero infection states and endemic equilibrium for which there are infected individuals [18], [20] and [21]. Better strategies can be formulated by determining conditions on the systems parameters leading to convergence to a disease-free equilibrium.

Multi-agent systems (MAS) are widely used to better understand complex systems through simulation. Indeed, solving complex problems requires a dynamic approach, it is no longer a question of calculating a solution from stable data but of maintaining an acceptable solution despite reorganizations and permanent disturbances. MAS are a response to those technical challenges and have demonstrated great potential in this context.

There are several factors to consider in the simulation of the current COVID-19 pandemic such as spatial and temporal variables that describe the context of the pandemic and different demographic and epidemiological properties of individuals. Agent-based modeling (ABM) makes it possible to efficiently cover all these subjects. For example, an agent can be easily used to model different categories of interactions constituting the social structure of the population, each with its own behavior, and its movements in a map over time. The agent's behavior is described by a set of rules that define the observed phenomenon. Since the

Journal of Theoretical and Applied Information Technology
30th September 2021. Vol.99. No 18

ISSN: 1992-8645 www.jatit.org E-ISSN: 1817-3195

COVID-19 outbreak, this approach proved to be very useful in modeling the spread of the disease and studying the effect of the different measures taken by governments [5], [17], [22] and [23].

COVID-19 spread modeling, in general, has been the subject of many recent articles and surveys [11], [24], [25] and [26]. The spread dynamic of COVID-19 belongs to a more general class of influenza disease outbreaks. The reader is referred to [27] where an SLIAR model is presented. Under this model, the waiting times in all compartments have been assumed to be exponential random variables. As we will see in the next section, this hypothesis does not represent correctly COVID-19 spreading dynamics and we will explain how a sojourn time closer to real dynamics can be introduced. A very fundamental scientific question is the influence of mobility on the qualitative behavior of the disease spread. A general review of migration, mobility and spatial-temporal spread of infectious pathogens of humans is given in [28]. We will use the approach proposed by Yang, C. and Wilensky [29] of the "Center for Connected Learning and Computer-Based Modeling, Northwestern University, Evanston, IL", in which a NetLogo framework provides a modeling environment for the development of free multi-agent systems.

In the present work, we assume that due to migration, external infected people join the population. And one of the main goals of the work is to visualize and illustrate quantitatively the influence of that phenomena by comparing analytical and numerical results in both closed and opened populations. Mobility will be represented by constant rates in the differential equation, and the model that have been developed by the authors, in NetLogo, integrates the possibility of applying one or more measures to slow the spread of the pandemic and to analyze the impact on the effective reproduction rate R_t, the duration of the pandemic or the mobility parameters.

Software developed by the authors, in sections **4** and **5**, simulates the disease spread using real parameters declared by the ministry of public health in Morocco. More precisely, a Runge-Kutta 4th order method using NetLogo is used to illustrate the system's behavior by solving numerically the ordinary differential equation governing the model. And then, an agent-based program has been developed to represent the epidemic dynamic for the same model. It should be noted that, here, we use different simulation approaches, for which parameters are not all the same, and consequently curves and values will not be identical. However, the two approaches lead to similar qualitative behavior conclusions.

In the next section, we present the proposed compartmental model. In section **3**, we establish the ordinary differential equation and determine the basic reproduction number as well as the final size relation. A detailed illustration of the theoretical results, in real data context, is the subject of section **4**. The parameters of the model related to a Moroccan case study will be estimated and the NetLogo software developed by the authors will be used to provide numerical simulations of the disease spread and to compute characterizing values of the epidemiological situation such as the peak timing and the maximal prevalence. We present, in the fifth section, the adopted multi-agents approach, considering the same model. Simulations under multi-agents methods support the observed results of section **3**. The method subject of the present work is discussed and analysed in section 6. We will conclude the paper with some remarks, recommendations and perspectives.

2. THE PROPOSED MODEL

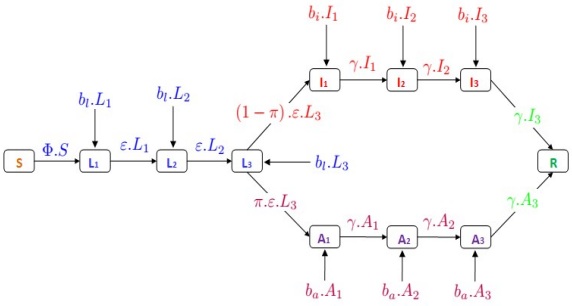

Figure 1: The Model Subject Of This Article

In the this work, we establish a general model of COVID-19 spread taking into account migration of new infected individuals into a population. In this paper, each infected compartment is subdivided into three sub-compartments instead of two. We have restricted our study to the case where migration rates are positive numbers less or equal to output rates. We assume that migration have not a considerable influence on the susceptible "S" and the recovered "R" compartments sizes. Those two hypotheses are compatible with the context of

COVID-19 studies. First, because, in general, governments control migration to infected cities and, thus, migration rates are relatively small. Second, because the survey time for such pandemic is less or equal to one year, therefore non infected compartments sizes can be assumed to be constant.

Moreover, sojourn times in the three are assumed to be Erlang random variables as mentioned by Arino et al in [11], the considered Erlang random variables have as "shape" n=2. In the present work, we take n=3, for the three infected states, so as to illustrate the influence of the "shape" values on the model and also in order to provide a distribution closer to real life data. Namely, and as in the model of [11], there are symptomatic and asymptomatic infective individuals. Moreover, before becoming infective, susceptible individuals become first latently infected such that the infected individuals in the latent compartment L_1 are carrying the virus but not yet transmitting it while the infected ones from the L_2 and L_3 compartments are infectious. The mean sojourn time in the combined incubation compartments, L_1, L_2 and L_3 is equal to $\frac{3}{\varepsilon}$, where ε is the rate at which incubation ends.

Likewise, the mean sojourn time in combined compartments I_1, I_2 and I_3, and in the combined compartments A_1, A_2 and A_3 are equal to $\frac{3}{\gamma}$, where γ is the recovery rate. As illustrated in Figure 1, b_l, b_a and b_i represent the migration rates to every latent, asymptomatic and symptomatic compartment respectively. They are, in general, not equal and they depend on the epidemiological structure of external populations. In addition, since symptomatic individuals are more detectable than asymptomatic and incubating cases, one should have $b_l > b_a > b_i$. However, we do not impose, in this work, any condition on migration rates ordering. The infectious latent states (L_2 and L_3) are less infective than the symptomatic states, their infectivity is therefore attenuated by a factor η. Likewise, we denote ξ the attenuation factor for transmission by asymptomatic cases. Here, we consider a mass action incidence with transmission coefficient β. Hence, the incidence takes the expression

$$\Phi.S = \beta.((I_1 + I_2 + I_3) + \xi.(A_1 + A_2 + A_3) + \eta.(L_2 + L_3)).S$$

3. MODEL ANALYSIS

A simple analysis of the model's dynamic leads to the ordinary differential equation (ODE):

$$\begin{cases} L_1' = \beta.((I_1 + I_2 + I_3) + \xi.(A_1 + A_2 + A_3) + \eta.(L_2 + L_3)).S - (\varepsilon - b_l).L_1 \\ L_2' = \varepsilon.(L_1 - L_2) + b_l.L_2 \\ L_3' = \varepsilon.(L_2 - L_3) + b_l.L_3 \\ I_1' = (1-\pi).\varepsilon.L_3 - (\gamma - b_i).I_1 \\ I_2' = \gamma.(I_1 - I_2) + b_i.I_2 \\ I_3' = \gamma.(I_2 - I_3) + b_i.I_3 \\ A_1' = \pi.\varepsilon.L_3 - (\gamma - b_a).A_1 \\ A_2' = \gamma.(A_1 - A_2) + b_a.A_2 \\ A_3' = \gamma.(A_2 - A_3) + b_a.A_3 \\ S' = -\beta.((I_1 + I_2 + I_3) + \xi.(A_1 + A_2 + A_3) + \eta.(L_2 + L_3)).S \\ R' = \gamma.(I_3 + A_3) \end{cases} \quad (3.1)$$

The suitable framework here is the method by P.van den Driessche and J. Watmough in [30]. With notations of section 2 in [30], we have

$x = (L_1, L_2, L_3, I_1, I_2, I_3, A_1, A_2, A_3, S, R)$,

$f(x) = F(x) - V(x) = F(x) - (V^-(x) - V^+(x)) = F(x) + V^+(x) - V^-(x)$

and

$\Phi = \beta.((I_1 + I_2 + I_3) + \xi.(A_1 + A_2 + A_3) + \eta.(L_2 + L_3))$

with

$$F(x) = \begin{pmatrix} \Phi.S \\ 0 \\ \vdots \\ \vdots \\ \vdots \\ 0 \end{pmatrix}, \quad V(x) = \begin{pmatrix} (\varepsilon - b_l).L_1 \\ -\varepsilon.(L_1 - L_2) - b_l.L_2 \\ -\varepsilon.(L_2 - L_3) - b_l.L_3 \\ -(1-\pi).\varepsilon.L_3 + (\gamma - b_i).I_1 \\ -\gamma.(I_1 - I_2) - b_i.I_2 \\ -\gamma.(I_2 - I_3) - b_i.I_3 \\ -\pi.\varepsilon.L_3 + (\gamma - b_a).A_1 \\ -\gamma.(A_1 - A_2) - b_a.A_2 \\ -\gamma.(A_2 - A_3) - b_a.A_3 \\ \Phi.S \\ -\gamma.(I_3 + A_3) \end{pmatrix}$$

$$V^-(x) = \begin{pmatrix} \varepsilon.L_1 \\ \varepsilon.L_2 \\ \varepsilon.L_3 \\ \gamma.I_1 \\ \gamma.I_2 \\ \gamma.I_3 \\ \gamma.A_1 \\ \gamma.A_2 + b_a.A_2 \\ \gamma.A_3 \\ \Phi.S \\ 0 \end{pmatrix}, \quad V^+(x) = \begin{pmatrix} b_l.L_1 \\ \varepsilon.L_1 + b_l.L_2 \\ \varepsilon.L_2 + b_l.L_3 \\ (1-\pi).\varepsilon.L_3 + b_i.I_1 \\ \gamma.I_1 + b_i.I_2 \\ \gamma.I_2 + b_i.I_3 \\ \pi.\varepsilon.L_3 + b_a.A_1 \\ \gamma.A_1 + b_a.A_2 \\ \gamma.A_2 + b_a.A_3 \\ 0 \\ \gamma.(I_3 + A_3) \end{pmatrix}$$

Theorem 3.1. The basic reproduction number of the model governed by equation 3.1 is $R_0 = R_l + R_I + R_A$, where

$$R_l = \beta.S(0).\left(\frac{\eta.\varepsilon}{(\varepsilon - b_l)^2} + \frac{\eta.\varepsilon^2}{(\varepsilon - b_l)^3}\right)$$

$$R_I = \beta.S(0).\left(\frac{(1-\pi).\varepsilon^3}{(\varepsilon-b_l)^3(\gamma-b_l)} + \frac{\gamma(1-\pi).\varepsilon^3}{(\varepsilon-b_l)^3(\gamma-b_l)^2} + \frac{\gamma^2(1-\pi).\varepsilon^3}{(\varepsilon-b_l)^3(\gamma-b_l)^3}\right)$$

Journal of Theoretical and Applied Information Technology
30th September 2021. Vol.99. No 18

ISSN: 1992-8645 www.jatit.org E-ISSN: 1817-3195

and

$$R_A=\beta.S(0).\left(\frac{\xi\pi\varepsilon^4\gamma^2(1-\pi)}{(\varepsilon-b_l)^3(\gamma-b_l)^3(\gamma-b_a)}+\frac{\xi\pi\varepsilon^4\gamma^3(1-\pi)}{(\varepsilon-b_l)^3(\gamma-b_l)^3(\gamma-b_a)^2}+\frac{\xi\pi\varepsilon^4\gamma^4(1-\pi)}{(\varepsilon-b_l)^3(\gamma-b_l)^3(\gamma-b_a)^3}\right).$$

The model has one disease free equilibrium $x_0=(0,0,0,0,0,0,0,0,0,S_\infty,R_\infty)$.

If $R_0<1$, then x_0 is locally asymptotically stable.
If $R_0>1$, then x_0 is unstable.

Proof. Let first prove that assumptions (A1)-(A5) of Theorem 2 of [30] are fulfilled.

It is clearly seen that if $x\geq 0$ then, $F(x)\geq 0, V^+(x)\geq 0$ and $V^-(x)\geq 0$. Hence (A1) is satisfied.

For all $i=1,2,\ldots,11$, if $x_i=0$ then $V_i^-(x)=0$ and thus (A2) is fulfilled.

For all $i>m=9$, we have $F_i=0$. Thus (A3) is satisfied.

If $x\in X_S$, then $x_i=0$ for all $i=1,2,\ldots,9$. Thus $F(x)=0$ and $V^+(x)=0$. Thus (A4) holds.

Let verify (A5).

Take the disease-free equilibrium $x_0=(0,0,0,0,0,0,0,0,0,S_\infty,R_\infty)$. If $F(x)=0$ is set to 0, then $Df(x_0)=-DV(x_0)$.

It is clearly seen that the Jacobian matrix of V at x_0 is a lower triangular matrix and $Diag(DV(x_0))=(\varepsilon-b_l,\varepsilon-b_l,\varepsilon-b_l,\gamma-b_l,\gamma-b_l,\gamma-b_l,\gamma-b_a,\gamma-b_a,\gamma-b_a,0,0)$

Thus $Sp(DV(x_0))=\{\varepsilon-b_l,\varepsilon-b_l,\varepsilon-b_l,\gamma-b_l,\gamma-b_l,\gamma-b_l,\gamma-b_a,\gamma-b_a,\gamma-b_a,0,0\}$. As pointed out in section 2, the study is restricted to the case where migration rates are less or equal to recovery rates. Mainly, $b_l\geq\varepsilon, b_a\geq\gamma$ and $b_i\geq\gamma$. Consequently, all eigenvalues of $DV(x_0)$ are real positive numbers and then all eigenvalues of $Df(x_0)$ are negative real number if $F(x)$ is set to 0. Completing the proof of (A5).

With notations of [30], we recall that $F=\left(\frac{\partial F_i}{\partial x_j}(x_0)\right)_{1\leq i,j\leq 9}$ and $V=\left(\frac{\partial V_i}{\partial x_j}(x_0)\right)_{1\leq i,j\leq 9}$.

We obtain

$$F=\beta.S_0.\begin{pmatrix}0&\eta&\eta&1&1&1&\xi&\xi&\xi\\0&\cdots&&\cdots&&\cdots&\cdots&0\\\vdots&&&&&&&\vdots\\0&\cdots&&\cdots&&\cdots&\cdots&0\end{pmatrix}$$

And

$$V=\begin{pmatrix}\varepsilon-b_l&0&\cdots&&\cdots&&\cdots&0\\-\varepsilon&\varepsilon-b_l&\ddots&&&&&\vdots\\0&-\varepsilon&\varepsilon-b_l&&&&&\\\vdots&\ddots&-(1-\pi)\varepsilon&\gamma-b_l&\ddots&&&\\-&&&-\gamma&\gamma-b_l&&&\vdots\\\vdots&&&\ddots&-\gamma&\gamma-b_l&\ddots&\\&&&&&-\pi\varepsilon&\gamma-b_a&\ddots&\vdots\\\vdots&&&&&\ddots&-\gamma&\gamma-b_a&0\\0&\cdots&&\cdots&&0&-\gamma&\gamma-b_a\end{pmatrix}$$

Now, theorem 2 of [30] applies and the basic reproduction number is $R_0=\rho(F.V^{-1})$, the spectral radius of the matrix $F.V^{-1}$.

It should be noted that explicit expression of V^{-1} exists (using a simple Maple worksheet) but very voluminous. We avoided including it here for reasons of simplicity. $F.V^{-1}$ has the form

$$\begin{pmatrix}\alpha&X&\cdots&\cdots&\cdots&\cdots&X\\0&\cdots&&\cdots&\cdots&\cdots&0\\\vdots&&&&&&\vdots\\0&\cdots&&\cdots&\cdots&\cdots&0\end{pmatrix}$$

Where

$$\alpha=\beta.S(0).\left(\frac{\eta.\varepsilon}{(\varepsilon-b_l)^2}+\frac{\eta.\varepsilon^2}{(\varepsilon-b_l)^3}+\frac{(1-\pi).\varepsilon^3}{(\varepsilon-b_l)^3(\gamma-b_l)}+\frac{\gamma(1-\pi).\varepsilon^3}{(\varepsilon-b_l)^3(\gamma-b_l)^2}+\frac{\gamma^2(1-\pi).\varepsilon^3}{(\varepsilon-b_l)^3(\gamma-b_l)^3}\right)+$$
$$\beta.S(0).\left(\frac{\xi\pi\varepsilon^4\gamma^2(1-\pi)}{(\varepsilon-b_l)^3(\gamma-b_l)^3(\gamma-b_a)}+\frac{\xi\pi\varepsilon^4\gamma^3(1-\pi)}{(\varepsilon-b_l)^3(\gamma-b_l)^3(\gamma-b_a)^2}+\frac{\xi\pi\varepsilon^4\gamma^4(1-\pi)}{(\varepsilon-b_l)^3(\gamma-b_l)^3(\gamma-b_a)^3}\right).$$

Then we have $Sp(F.V^{-1})=\{0,\alpha\}$. Thus, $R_0=\rho(F.V^{-1})=\alpha$.

A better expression of R_0 is $R_0=R_l+R_I+R_A$ where

$$R_l=\beta.S(0).\left(\frac{\eta.\varepsilon}{(\varepsilon-b_l)^2}+\frac{\eta.\varepsilon^2}{(\varepsilon-b_l)^3}\right)$$

$$R_I=\beta.S(0).\left(\frac{(1-\pi).\varepsilon^3}{(\varepsilon-b_l)^3(\gamma-b_l)}+\frac{\gamma(1-\pi).\varepsilon^3}{(\varepsilon-b_l)^3(\gamma-b_l)^2}+\frac{\gamma^2(1-\pi).\varepsilon^3}{(\varepsilon-b_l)^3(\gamma-b_l)^3}\right)$$ and

$$R_A=\beta.S(0).\left(\frac{\xi\pi\varepsilon^4\gamma^2(1-\pi)}{(\varepsilon-b_l)^3(\gamma-b_l)^3(\gamma-b_a)}+\frac{\xi\pi\varepsilon^4\gamma^3(1-\pi)}{(\varepsilon-b_l)^3(\gamma-b_l)^3(\gamma-b_a)^2}+\frac{\xi\pi\varepsilon^4\gamma^4(1-\pi)}{(\varepsilon-b_l)^3(\gamma-b_l)^3(\gamma-b_a)^3}\right).$$

Remark 1. In the absence of migration i.e $b_i=b_a=b_l=0$, we obtain the basic reproduction number established in [11] where the population has been assumed to be closed:

$$R_0=\beta.S(0).\left(2\frac{\eta}{\varepsilon}+3\frac{1-\pi}{\gamma}+3\frac{\xi\pi\varepsilon(1-\pi)}{\gamma^2}\right)$$

The final size relation will be determined, only in the case of a closed population, using Theorem 1.5 of [31]. For reader convenience, we recall its integral text. Unfortunately, the theorem cannot be applied to the case of a population opened to migration.

Theorem 1.5 in [31]
Consider the epidemic model

$$\begin{cases} x' = \beta(x,y,z).\Pi.D.b.x - V.x \\ y' = g(x,y,z) - \beta(x,y,z).D.y.b.x \\ z' = h(x,y,z) + W.x \end{cases} \quad (3.2)$$

Then $x_\infty = 0$ and the final size relation is given by

$$\frac{1}{\sigma_i}\ln\left(\frac{y_i(0)}{y_i(\infty)}\right) = \beta b.V^{-1}.\Pi(y(0)-y(\infty)) + \beta b.V^{-1}.x(0) \quad (3.3)$$

if $y_i > 0$.

The theorem bellow provides the final size relation.

Theorem 3.2. Assume in equation 3.1 that $b_i = b_a = b_l = 0$. The final size relation is given by:

$$\ln\left(\frac{S_0}{S_\infty}\right) = \frac{R(0)}{S_0}.(S_0 - S_\infty) + \beta b.V^{-1}.x(0) \quad (3.4)$$

Where

$[x(0)]^T = (L_1(0), L_2(0), L_3(0), I_1(0), I_2(0), I_3(0), A_1(0), A_2(0), A_3(0))$,

$S_\infty = \lim_{t\to+\infty} S(t)$ and $S_0 = S(0)$.

Proof. In the present context we have:

$$\ln\left(\frac{y(0)}{y(\infty)}\right) = \frac{R(0)}{y(0)}.(y(0) - y(\infty)) + \beta.b.V^{-1}.x(0)$$

Then, with the notations of the paper, we have the final size relation

$$\ln\left(\frac{S_0}{S_\infty}\right) = \frac{R(0)}{S_0}.(S_0 - S_\infty) + \beta b.V^{-1}.x(0)$$

Where $S_0 = S(0)$ is the initial number of susceptible individuals in the population, and

$[x(0)]^T = (L_1(0), L_2(0), L_3(0), I_1(0), I_2(0), I_3(0), A_1(0), A_2(0), A_3(0))$,

represents all initially infected individuals.

$S_\infty = \lim_{t\to+\infty} S(t)$ is the final size of the susceptible compartment.

4. NUMERICAL SIMULATIONS USING THE ODE APPROACH

In this section, we focus on a real case study by considering the Moroccan context of COVID-19. Our parameters estimation will be based on the official report of the publish health ministry published on 05/01/2021. More precisely, we have three principal objectives:

1) Determining all system's parameters for the considered population.
2) Forecasting the epidemiological situation of COVID-19 in the period after 05/01/2021 with numerical simulations using a Runge-Kutta 4th Order Method implemented in "NetLogo" software
3) Studying and illustrating the influence of migration on the qualitative behaviour of the disease.

Let's start by setting the values of "universal" parameters. The mean incubation time has been the subject of many works [31], [32] and [33]. We take 6.8 days as a mean incubation period, the value estimated by C. Eliaset al. in [32].

That is $\frac{3}{\varepsilon} \approx 6.8$ days i.e $\varepsilon \approx \frac{3}{6.8} \approx 0.44$. Likewise, the length of infection is $\frac{3}{\gamma} \approx 8$ days. Thus $\gamma \approx \frac{3}{8} \approx 0.375\ \text{day}^{-1}$.

From real data published by the moroccan public health ministry, the fraction of asymptomatic cases in the study period is about $\pi = 0.9$ and the basic reproduction number is $R_0 = 0.8$.

We take as attenuation factors $\xi = 0.4$ and $\eta = 0.1$ as mean values from the table published in [11]. We recall that, up to now, there are no precise values for those two parameters. The total population size of Casablanca city is about $\tilde{N}=6.10^6$.

In this section, we will simulate the evolution of the disease spread under the following

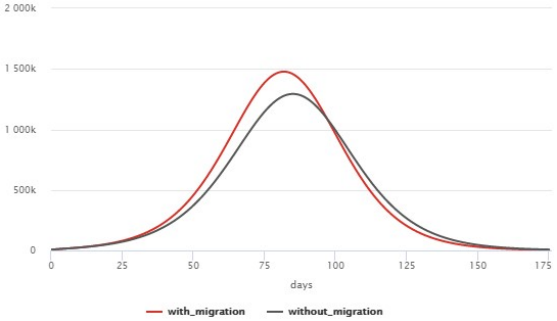

Figure 2: NetLogo(ODE): All Infected Cases $\sum_{i=1}^{3}(L_i + I_i + A_i)$

estimated initial values $I_1(0) = 3.10^3, I_2(0) = 12.10^2, I_3(0) = 18.10^2, S(0) = \tilde{N} - 6.10^3$

$$A_1(0) = A_2(0) = A_3(0) = L_1(0) = L_2(0) = L_3(0) = R(0) = 0$$

Then, from the formula

$$R_0 = \beta.S(0).\left(2\frac{\eta}{\varepsilon} + 3\frac{1-\pi}{\gamma} + 3\frac{\xi\pi\varepsilon(1-\pi)}{\gamma^2}\right),$$

we deduce that $\beta \approx 8.3811.10^{-8}$.

Journal of Theoretical and Applied Information Technology
30th September 2021. Vol.99. No 18

ISSN: 1992-8645 www.jatit.org E-ISSN: 1817-3195

We also recall that our goal is, principally, to set up a practical framework based on the dynamical systems approach, applicable to other epidemiological contexts.

Figures 2,3,4 and 5 provides a comparison between the epidemiological situations with and without migration provided by numerical simulations with "NetLogo" programming language.

In the absence of migration and for symptomatic cases, the peak is reached at the 88.6th day with maximal prevalence 70206. While the general number of all infected

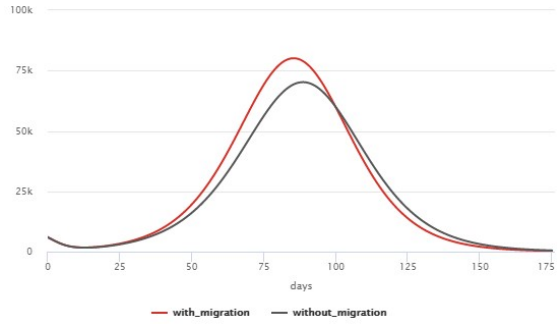

Figure 3: NetLogo(ODE): Symptomatic Cases $\sum_{i=1}^{3} I_i$

individuals $\sum_{i=1}^{3}(L_i+I_i+A_i)$ reaches its maximal value 1292943 in the 85th day.

After considering migration to the infected compartments with factors $b_l = b_a = 0.005$ and $b_i = 0.001$. The basic reproduction number increases from 0.8, in the absence of migration, to 0.835.

Numerical simulations provide all the values characterizing the disease spread under migration. A complete comparison is provided in Table 1.

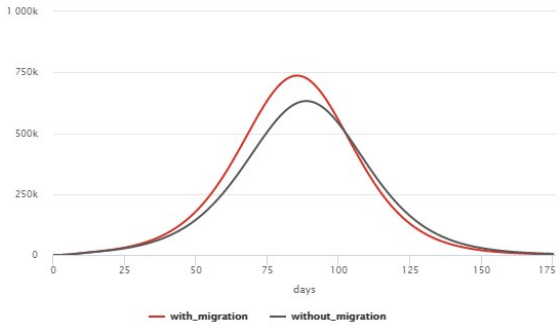

Figure 4: NetLogo(ODE): Asymptomatic Cases $\sum_{i=1}^{3} A_i$

Table 1: Summary Of The Results Of the First Approach

Characterizing values	Closed population	Opened population
The basic reproduction number R_0	0.8	0.835
The timing of the symptomatic peak	88.6th day	85.3th day
The timing of the general infection peak	85th day	81.8th day
The prevelance at the symptomatic peak	70206	80104
The prevelance at the general infection peak	1292943	1477192

As we see, migration causes an augmentation of the prevalence at the general infection peak, the prevalence at the symptomatic peak and the basic reproduction number R_0. It causes also a diminution of the timing of the general infection peak and the timing of the symptomatic peak.

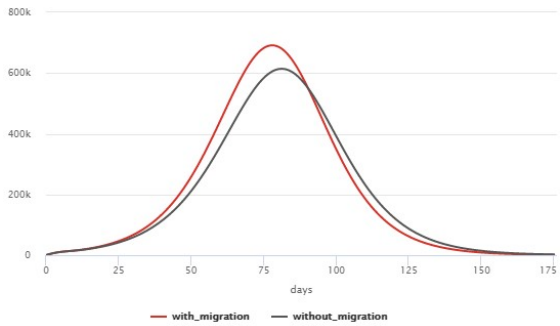

Figure 5: NetLogo(ODE): Latent Cases $\sum_{i=1}^{3} L_i$

5. NUMERICAL SIMULATIONS USING MULTI-AGENTS APPROACH

In this section, the same model as in Figure 1 will be implemented using a multi-agent approach in NetLogo. Unfortunately, we cannot simulate the previous system, for the total population size $\tilde{N}=6.10^6$, under our MAS technical conditions. Consequently, we have reduced, in this section, the total population size $\tilde{N}$ to $N= 10^4$. It should be noted that many parameters of ODE approach have not the same signification in MAS. Consequently, we define our private values in this section as in Table 2.

Journal of Theoretical and Applied Information Technology
30th September 2021. Vol.99. No 18

ISSN: 1992-8645 www.jatit.org E-ISSN: 1817-3195

Table 2: Parameters Of MAS's Input

Parameters	Values
The infection probability	0.05
The probability of being asymptomatic π_n	0.9
The average incubation period	6 days
The average infectious period	3 days

To quantify the intensity of the epidemic outbreak in this approach, the effective reproduction number R_t is computed at each iteration.

In order to model the effect of migration on the spread of the pandemic two scenarios will be studied. The migration of individuals is prohibited in the first one but is allowed in the second scenario with the following migration rates: $b_l = 0.005$ in each L sub-compartment, $b_a = 0.005$ in each A sub-compartment and $b_i = 0.001$ in each I sub-compartment.

Figures 6,7,8,9 and 10 provides a comparison between the epidemiological situations with and without migration using the multi-agent approach with "NetLogo" programming language. In the absence of migration, the peak for the symptomatic cases is reached at the 24.7th day with a maximal prevalence of 583 infected and the general number of all infected individuals reaches its maximal value 8273 in the 22th day. Whereas when migration is allowed, the peak of the symptomatic infected is 590 and the peak of all infected individuals is 8616. After allowing the migration into the infected compartments, the peak of the asymptomatic cases increases from 4946 on the 24th day to 5364. Which means that a higher peak is reached in each infected compartment due to migration. The effective reproduction number also increases due to migration from 3.80 to 4.10. The results of the simulations are summarized in Table 3.

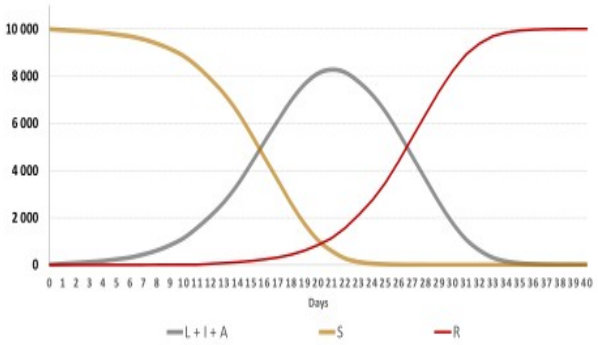

Figure 6: NetLogo (MAS) First Scenario: Without Migration

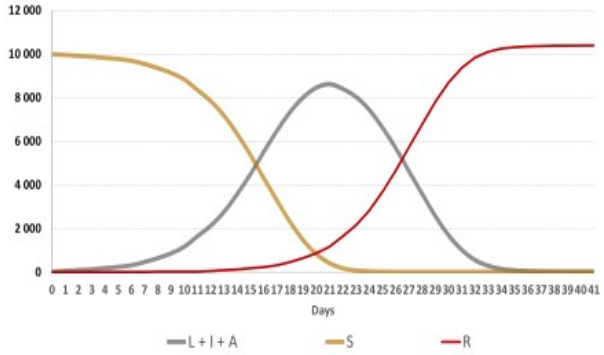

Figure 7: NetLogo(MAS) Second Scenario:With Migration

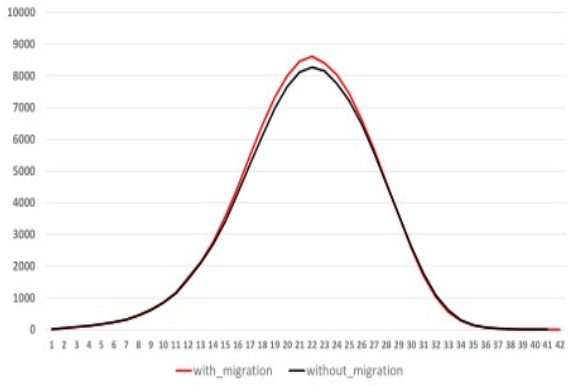

Figure 8: NetLogo(MAS): All Infected Cases

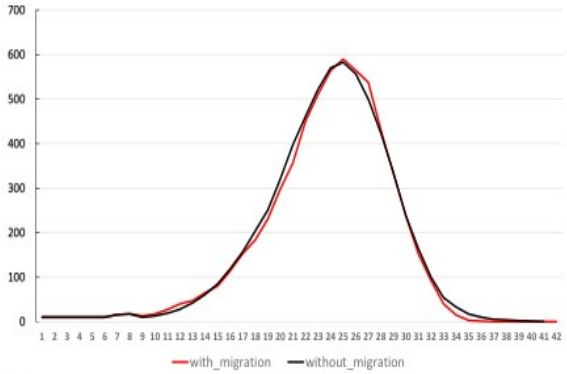

Figure 9: NetLogo(MAS): Symptomatic Cases

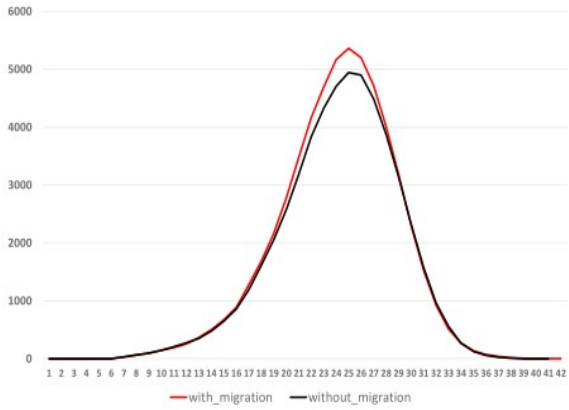

Figure 10: NetLogo(MAS): Asymptomatic Cases

Table 2: Summary Of The Results Of the Second Approach

Characterising values	Closed population	Opened population
The peak of the effective reproduction number R_t	3.80	4.10
The timing of the symptomatic peak	24.7th day	24th day
The timing of the general infection peak	22th day	21th day
The prevelance at the symptomatic peak	583	590
The prevelance at the general infection peak	8273	8616

The migration increases the peak of infected cases as well as that of the reproduction number. As a result, the disease spreads faster and more widely due to migration.

6. DISCUSSION AND ANALYSIS OF THE PROPOSED METHOD:

Based on the works developed in [11], [30] and [31], we propose in this paper, a new compartmental COVID-19 epidemiological model using eleven compartments and Erlang sojourn times. In order to validate our model and also to offer a complete and efficient decision support tool, we used two complementary approaches. Indeed, the dynamical systems or ODE approach is used to understand how the epidemic evolves in the whole population, by simulating the evolution of the infection in the compartments. This approach differs from the proposed multi-agent based (MAB) one which makes it possible to follow the evolution of the infection in a microscopic level. The proposed model takes into account the mobility phenomena and illustrates it quantitatively. We have proved that the dynamic of the disease is governed by an ordinary differential equation. All coefficients and rates have been defined and interpreted. Using the framework settled in [31], the final size relation has been obtained for closed population. The basic reproduction number, for a population with migration, has been determined using the approach published in [31]. It has been observed that the system with migration models a closed population (without mobility) under the assumption $b_i = b_a = b_l = 0$, and that it provides a quantitative representation of migration influence on the disease spread properties. This observation has been clearly illustrated by the numerical simulations using the "NetLogo" software developed by the authors. As we have explained, we assume that infected external people can join the population. One of our goals is to visualize and illustrate quantitatively the influence of this mobility, by comparing analytical and numerical results in closed and open populations. Mobility is represented by constant rates in the differential equation, and the MAB model developed in NetLogo, incorporates the possibility of applying one or more measures to slow the spread of the pandemic and analyze the impact on the reproduction rate R_t, duration of the pandemic or mobility parameters. We observed in the simulations made by the two approaches (ODE and MAB), that the mobility leads to an increase in the basic reproduction number R_0, the prevalence at the general infection peak and the prevalence at the symptomatic peak. Conversely, it causes a remarkable decrease in the values of the total duration of infection, the timing of the general infection peak and the timing of the symptomatic

peak. According to the simulations carried out by the proposed model, it can be seen that the opening of society to migration leads to the spread of diseases increasing and to reaching the epidemic peak more quickly. It should be noted that due to technical constraints, we were obliged to reduce the total size of the population to $N=10^4$ for the multi-agent simulation. However, both approaches provide the same qualitative and quantitative descriptions.

7. CONCLUSION

In this work we seek to provide a decision support tool for planners of public health policies in the event of a pandemic. Indeed, based on a realistic model taking into account the possibility of migration, we establish an explicit formula for the calculation of the basic reproduction number, and we succeed in obtaining a residence time quite close to the times observed experimentally [11].
This model provides an effective tool for decision makers to control the spread of the disease at a reasonable and realistic migration rate. And this means that a calculable minimum level of migration rates can be allowed to avoid any moving excessive deterioration of the epidemiological situation.

We have proved that the dynamic of the disease is governed by an ordinary differential equation and all coefficients and rates have been defined and interpreted. We have used our ameliorated SLIAR model with eleven compartments to show how the disease properties change with migration of new infected individuals into the population. It has been shown, using the framework in [31], that the final number of susceptible individuals for a closed population depends on initial conditions and on the system parameters implicitly via the equation in Theorem 3.2. Unfortunately, the method in [31] cannot be used to compute the final size relation for an open population.

Moreover, under the mobility scenario, with linear inputs, it has been shown that the basic reproduction number is the sum of three decreasing sub-reproduction numbers R_I, R_L and R_A which are decreasing functions of $(\varepsilon-b_i)^2$, $(\gamma-b_l)^2$ and $(\gamma-b_a)^2$. Consequently, R_0 is an increasing function of b_i, b_l and b_aWe can therefore conclude that the possibility of migration leads to reinforce the spread of diseases and to reach the epidemic peak very quickly. Simulating the model using the MAB approach for the real size of the population of Casablanca city, $\tilde{N}=6.10^6$, will be the subject of future work.

For reader's convenience, we summarize the main features of the proposed method. First, our approach is hybrid and illustrates the results using two different approaches. Second, the consideration of three compartments for each infection state provides a modeling process closer to experimental observed sojourn times [11]. Moreover, the explicit formula of the basic reproduction number provides an efficient tool for decision makers to control the disease spread under reasonable and realistic migration rates. And that means that a computable minimum level of freedom of movement can be allowed while avoiding excessive deterioration of the epidemiological situation. The proposed method provides also the values of all important dates in the dynamic of the model.

A detailed study of conditions on b_i, b_a and b_l leading to $R_0 < 1$ can be the subject of interesting coming papers. Such works can provide interesting three-dimensional $R_0 < 1$ zones. Future work can also be focused on more sophisticated representations of migration incidence which is not in many contexts linear. Moreover, it could be interesting to establish a fractional version of the model studied here, with adequate theoretical analysis and numerical simulations [35].
The obtained results show that the dynamical systems framework for compartmental epidemiological models is an efficient tool for forecasting the evolution of the disease. And the mathematical analysis illustrated by adequate software provides useful indicators to the decision makers.

ACKNOWLEDGMENT:

This work is supported by the CNRST and Mohammed V University in Rabat, project: Mathematical modeling and artificial intelligence for the analysis of the evolution of the Coronavirus pandemic in Morocco.

REFERENCES:

[1] Calafiore G.C, Novara C and Possieri C, "A modified SIR model for the COVID-19 contagion in Italy." 2020 59th IEEE Conference on Decision and Control (CDC). IEEE, 2020.

[2] Dashtbali M and Mirzaie M, A compartmental model that predicts the effect of social distancing and vaccination on controlling COVID-19. Sci Rep 11, 8191 (2021). https://doi.org/10.1038/s41598-021-86873-0.

[3] Li M.Y, An introduction to mathematical modeling of infectious diseases, Mathematics of planet earth, volume 2, Springer International Publishing AG 2018.

[4] Ma Z and Li J, Dynamical Modeling and Analysis of Epidemics. By World Scientific Publishing Co. Pte. Ltd. 2009.

[5] Petronio C.L.S, Paulo V.C.B, Helderet S.L et al. COVID-ABS: An agent-based model of COVID-19 epidemic to simulate health and economic effects of social distancing interventions, ChaosSolitons and Fractals, Volume 139, October 2020.

[6] Ian Cooper, Argha Mondal, Chris G, Antonopoulos. A SIR model assumption for the spread of COVID-19 in different communities, Chaos, Solitons & Fractals, Volume 139, 2020.

[7] Chen, Yi-Cheng, et al. "A time-dependent SIR model for COVID-19 with undetectable infected persons." IEEE Transactions on Network Science and Engineering 7.4 (2020): 3279-3294.

[8] Konstantin S. Sharov, Creating and applying SIR modified compartmental model for calculation of COVID-19 lockdown efficiency, Chaos, Solitons & Fractals, Volume 141, 2020.

[9] Moein S, Nickaeen N, Roointan A et al. Inefficiency of SIR models in forecasting COVID-19 epidemic: a case study of Isfahan. Sci Rep 11, 4725 (2021). https://doi.org/10.1038/s41598-021-84055-6

[10] Sharma S, Volpert V and Banerjee M, "Extended SEIQR type model for COVID-19 epidemic and data analysis." medRxiv (2020).

[11] Arino J and Portet S, A simple model for COVID-19, Infectious Disease Modelling Volume 5, 2020, Pages 309-315, doi: 10.1016/j.idm.2020.04.002

[12] Niu, Ruiwu, et al. "Modeling the COVID-19 pandemic using an SEIHR model with human migration." IEEE Access 8 (2020): 195503-195514.

[13] Batistela C.M, Correa D.P.F, Bueno A.M and Piqueira J.R.C, SIRSi compartmental model for COVID-19 pandemic with immunity loss, Chaos, Solitons & Fractals, Volume 142, 2021.

[14] Chen M, Li M, Hao Y, Liu Z, Hu L and Wang L, The introduction of population migration to SEIAR for COVID-19 epidemic modeling with an efficient intervention strategy, Information Fusion, Volume 64, 2020.

[15] Sirkeci I, and Yucesahin M.M. "Coronavirus and migration: analysis of human mobility and the spread of Covid-19." Migration Letters 17.2 (2020): 379-398.

[16] Bohner M, Streipert S and Torres D.FM, Exact solution to a dynamic SIR model, Nonlinear Analysis: Hybrid Systems, 32(2019),228-238.

[17] Zhang S and Zhou Y,The analysis and application of an HBV model, Applied Mathematical Modelling 36 (2012) 13021312.

[18] Yan P and Chowell G, Quantitative methods for Investigating infectious disease outbreaks,Crown 2019.

[19] Brauer F, Mathematical epidemiology past present and future, Infectious Disease Modelling, pp. 113-127, 2017.

[20] Brauer F, Van den Driessche P and Wu J, Mathematical Epidemiology, Springer-Verlag Berlin Heidelberg, 2008.

[21] Brauer F, The Kermack-McKendrick epidemic model revisited, Mathematical Biosciences, Volume 198, Issue 2, pp. 119-131, December 2005.

[22] Bouchnita A and Jebrane A, A hybrid multi-scale model of COVID-19 transmission dynamics to assess the potential of non-pharmaceutical interventions,Chaos Solitons and Fractals,Volume 138,2020.

[23] Yaroslav V, Mykhailo M, Miroslav S et al. Modeling and analysis of different scenarios for the spread of COVID-19 by using the modified multi-agent systems-Evidence from the selectedcountries, Results in Physics, Volume 20,2021.

[24] Djilali S, Benahmadi L, Tridane A and Niri K, Modeling the Impact of Unreported Cases of the COVID-19 in the North African Countries, Biology, Volume 9, 2020.

[25] Gharakhanlou N. M, Hooshangi N, Spatio-temporal simulation of the novel coronavirus (COVID-19) outbreak using the agent-based modeling approach (case study: Urmia, Iran), Informatics in Medicine Unlocked, Volume 20, 2020.

[26] Vermeulen B, Pyka A, and Muller M, An agent-based policy laboratory for COVID-19 containment strategies, 2020.

[27] Arino J, Brauer F, Van den Driessche P, Watmough J and Wu J, Simple models for containment of a pandemic, J. R. Soc. Interface (2006) 3, 453-457.

[28] Arino J, Spatio-temporal spread of infectious pathogens of humans, Infectious Disease Modelling 2 (2017) 218-228.

[29] Yang C and Wilensky U, NetLogoepiDEM Travel and Control model, Center for connected learning and computer-based modeling, Northwestern University, Evanst, 2011.

[30] Van den Driessche P and Watmough J, Reproduction numbers and sub-threshold endemic equilibria for compartmental models of disease transmission, Mathematical Biosciences, 180 (2002) 29-48.

[31] Arino J, Braouer F, P. Van den Driessche P, Wathmogh J and Wu J, A final size relation for epidemic models, Mathematical Biosciences and engineering, Volume 4, Number 2, April (2007) 159-175.

[32] Eliasa C, Sekria A, Leblanca P, Cucheratc M and Vanhemsa P, The incubation period of COVID-19: A meta-analysis,International Journal of Infectious Diseases 104 (2021) 708-710.

[33] Ki M, Epidemiologic characteristics of early cases with 2019 novel coronavirus (2019-nCoV) disease in Korea, Epidemiology and health, Volume: 42, Article ID: e2020007.

[34] H. Lee, K. Kim, K. Choi, S. Hong, H. Son and S. Ryu, Incubation period of the coronavirus disease 2019 (COVID-19) in Busan, South Korea (in press: https://doi.org/10.1016/j.jiac.2020.06.018).

[35] Yusuf A, Qureshi S, M. Inc, Aliyu A. I, Baleanu D and Shaikh A.A, Two-strain epidemic model involving fractional derivative with Mittag-Leffler kernel, Chaos 28, 123121(2018).